INTL JOURNAL OF ELECTRONICS AND TELECOMMUNICATIONS, 2026, VOL. 72, NO. 2, PP. 1–7
Manuscript received November 19, 2025; revised April 2026. doi: 10.24425/ijet.2026.157934

# Enhanced High-Voltage power line insulator and contamination classification using score-level fusion

Balu Bhusari, Akshay Jadhav, and Balasaheb Balkhande

***Abstract*—High-voltage (HV) power line insulators are critical for grid reliability, but their performance degrades due to contamination (e.g., salt, soot, excrement). Traditional visual inspection methods are subjective, risky, and time-consuming. To overcome these challenges, this paper proposes an efficient and accurate framework for classifying insulator materials (glass, porcelain, composite) and contamination types. The framework employs features extracted independently from three lightweight CNNs: MobileNetV2, ShuffleNet, and EfficientNet-B0. These features are then fed into base classifiers, and their outputs (scores) are combined using various score-level fusion rules (Majority Vote, Maximum, Average, Sum, Minimum, Product) to enhance classification accuracy and robustness. The framework's effectiveness is validated on three datasets, including synthetic contamination scenarios and real-world images from the Merged Public Insulator Dataset (MPID). Results demonstrate that score fusion significantly outperforms individual lightweight models, achieving accuracies up to 98.49% for contamination classification, 98.59% for combined material/contamination classification, and 99.26% for real-world material identification. Comparative analysis demonstrates significant improvements over existing methods, including VGG16 (97.00%) and custom CNNs (98.00%), highlighting the efficacy of feature and score fusion. The results validate the framework's adaptability to diverse environments, computational efficiency, and potential for deployment in resource-constrained settings.**

***Keywords*—high-voltage power line insulator; Score-based classifier fusion; light-weight CNN; insulator contamination; transfer learning feature fusion**

## I. Introduction

HIGH-VOLTAGE (HV) power lines are the backbone of modern electricity transmission systems, responsible for delivering electricity from power generation plants to substations and end-users with minimal energy loss [1]. The reliability of these systems is critical for ensuring a consistent and uninterrupted power supply, especially as the demand for electricity continues to grow globally. High-voltage insulators are essential components of these power lines, providing both electrical insulation and mechanical support to the conductors [2]. Insulators are typically made from materials such as glass, porcelain, or polymer composites, each offering unique properties that make them suitable for specific applications [3]. However, despite their robust design, insulators are susceptible to surface contamination, which can significantly degrade their performance over time.

Contamination on insulator surfaces can arise from various sources, including industrial pollution, salt deposits in coastal areas, and bird excrement. These contaminants can form a conductive layer on the insulator surface, especially under high humidity conditions, leading to increased leakage currents, arcing, and even flashovers [4]. Therefore, accurate classification of insulator types and contamination levels is crucial for effective maintenance and grid reliability. Traditional methods for assessing insulator conditions, such as visual inspections, are highly subjective, time-consuming, and prone to human error. Moreover, inspecting energized high-voltage power lines poses significant safety risks to personnel [5].

Initial techniques relied on traditional image processing algorithms, utilizing handcrafted features and rule-based classifiers. Pernebayeva et al. [6] proposed an image-based method for outdoor insulator surface evaluation, employing texture and color features. However, such methods struggled with complex backgrounds and varying lighting conditions, limiting their robustness in real-world scenarios. Multi-patch deep features are introduced for insulator status classification from aerial images, demonstrating the potential of CNNs in handling large-scale datasets [7]. Filho et al. [8] combined CNNs with SVMs, achieving 95% accuracy for defective insulator classification, though misclassification rates persisted for severely degraded ceramic insulators.

Recent studies have explored pre-trained CNN architectures like VGG, ResNet, and DenseNet for contamination classification. Picolotto Corso et al. [9] evaluated these models and found ResNet-50 to be the most effective, achieving 99.24% accuracy and an F1-score of 0.9743. Similarly, researcher in [10] utilized deep features from VggNet and GoogleNet with a random forest classifier, attaining 98.99% accuracy on a synthetic dataset. Ferraz et al. (2024) [11] employed VGG16, ResNet-34, and a custom CNN, achieving an average accuracy of 0.98 for cleanliness classification.

To mitigate computational costs, hybrid and lightweight models have been proposed. A CNN-based framework for UAV-captured insulator images is developed in [12], achieving 95.5% accuracy. Authors [13] combined edge detection with neural networks, reaching 97.50% accuracy for contaminated

Balu Bhusari is with Faculty of Electronics and Communication, Ramrao Adik Institute of Technology, DY Patil Deemed to be University, Navi Mumbai, India (e-mail: balu.bhusari@rait.ac.in, ORCID: 0000-0002-9596-7446).

Akshay Jadhav is with Faculty of Artificial Intelligence and Data Science, SIES Graduate School of Technology , Navi Mumbai, India (e-mail: aajadhav156@gmail.com).

Balasaheb Balkhande is with Faculty of Computer Engineering, Vasantdada Patil Pratishthan's College of Engineering and Visual Arts, Mumbai, India (e-mail: prof.balasahebwbalkhande@pvppcoe.ac.in, ORCID: 0000-0001-8685-8945).

insulator classification. Overall, two critical challenges persist: (1) conventional CNNs require extensive labeled datasets for training and incur substantial computational costs, and (2) their accuracy remains suboptimal for complex classification tasks involving diverse insulator materials and contamination patterns. To mitigate these limitations, current research has explored two parallel strategies: (1) lightweight CNN architectures and (2) transfer learning with feature fusion. These methodologies collectively address the trade-offs between computational efficiency and classification performance, offering scalable solutions for real-world power grid monitoring applications.

This article presents a new score-level classifier fusion framework for the classification of high-voltage power line insulators and their contamination levels. The proposed approach combines deep neural network feature fusion to classify insulator materials (ceramic, glass, and composite) and contaminants (salt, soot, bird excrement, and clean). The methodology involves extracting features from three pre-trained MobileNetV2, ShuffleNet and EfficientNet-B0 models, score-level classifier fusion algorithm to improve the classification accuracy. The framework is evaluated on three datasets, including both synthetic and real-world images of HV insulators and contaminants.

The major contributions of this study are as follows:

- The proposed method employs score-level classification strategy leading to improved classification accuracy.
- The algorithm employs fused deep features from MobileNetV2, ShuffleNet and EfficientNet-B0 to capture multi-scale texture and spectral patterns, enhancing insulators classification rate and demonstrating robustness in diverse environments.
- The framework is validated on three datasets, including synthetic and real-world (MPID) images, under various contamination scenarios, ensuring generalizability across different insulator materials and contamination types.

## II. Materials and Methods

### A. Database

The performance of the proposed score-based classifier fusion algorithm was rigorously evaluated using three distinct datasets derived from synthetic generation and real-world sources. The primary synthetic dataset, generated following the methodology in [2] comprises 14,424 images simulating common high-voltage insulator contaminants (salt, soot, bird excrement) alongside clean insulators across ceramic, polymeric, and glass materials. This dataset is carefully balanced, containing 3,606 images for each condition (including clean) and 1,202 images per insulator material within each condition.

Complementing this, real-world data was sourced from the Merged Public Insulator Dataset (MPID) [14] a large collection of drone-acquired inspection images captured under diverse conditions (e.g., time of day, season, weather, viewing angles, camera types) and featuring glass, porcelain, and composite insulators. The combined use of synthetic and real-world datasets ensures a comprehensive evaluation of the model's robustness and adaptability to varied operational scenarios. Specific details regarding the composition and characteristics differentiating the three datasets utilized (referred to herein as Database 1, Database 2 derived from [2], and Database 3 from MPID [14]) are illustrated in figure 1.

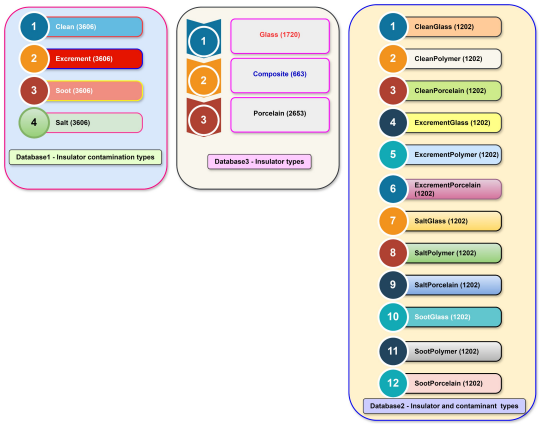


Fig. 1. Database details used in the current study.

### B. Method

The proposed framework is designed to classify high-voltage power line insulators and their contamination levels using a combination of light-weight Convolutional Neural Networks (CNNs), feature fusion, and classifier score fusion techniques. Figure 2 shows the framework of the proposed classification algorithm. The pre-processing stage ensures that the input images are standardized for further analysis. This involves image resizing to a uniform dimension, normalization, and augmentation to improve the robustness and generalization of the model.

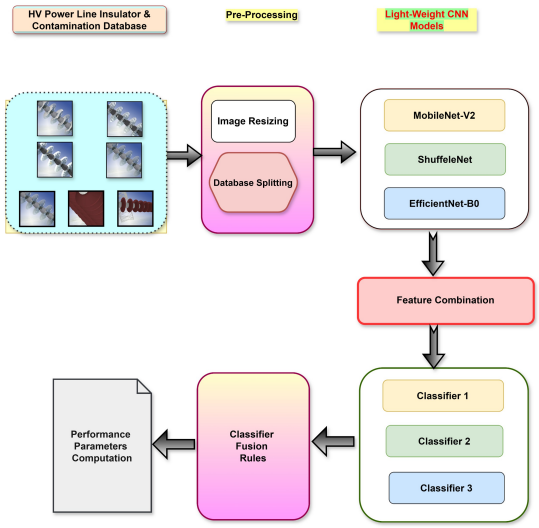


Fig. 2. Proposed HV power line insulator and contamination classification framework.

Three light-weight CNN architectures are employed for feature extraction: (1) MobileNetV2 (2) ShuffleNet and

(3) EfficientNet-B0. Each CNN model processes the pre-processed images independently, extracting distinct sets of features that capture different aspects of the insulator and contamination characteristics. Features extracted from deep learning models effectively important textural and color characteristics as explained in variety of applicatioms [15], [16]. The fusion step enhances the discriminative power of the system by integrating complementary information from multiple architectures. The dataset is divided into training and test sets to ensure unbiased model evaluation.

Key performance metrics such as accuracy, precision, recall, F1-score, and confusion matrices are computed to evaluate the effectiveness of the individual CNN models and the fused system. To further improve classification robustness, a classifier score fusion approach is employed. The predictions from three classifiers (corresponding to the three CNN models) are combined using fusion rules such as: (a) Majority Voting (b) Average (c) Minimum (d) Maximum (e) Product and (f) Sum. This step ensures that the strengths of each classifier are leveraged, mitigating individual model weaknesses and improving overall system reliability.

### C. Light-Weight CNN based feature extraction

Lightweight Deep Neural Networks are designed to address the high computational complexity of traditional CNN, making them suitable for resource-constrained devices.

EfficientNet-B0: EfficientNet-B0 is a family of convolutional neural networks (CNNs) optimized for both accuracy and computational efficiency [17]. Its innovation lies in compound scaling, a method that uniformly scales network depth, width, and resolution using a fixed set of coefficients. The architecture employs MBConv blocks, which combine inverted residual layers with squeeze-and-excitation (SE) modules. These blocks use depthwise separable convolutions to reduce parameters and emphasize important channels dynamically [18]. Subsequent variants (B1–B7) scale up the base model systematically, with higher-index models offering greater accuracy at increased computational costs.

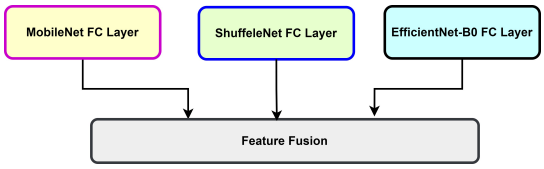


Fig. 3. Feature fusion of three light-weight CNN models.

MobileNetV2: MobileNetV2 is a family of lightweight convolutional neural networks designed for efficient deployment on mobile and embedded devices with limited computational resources [19]. MobileNetV2 employs depthwise separable convolutions to significantly reduce the number of parameters and computational cost while maintaining competitive accuracy [20]. These convolutions split the standard convolution into two operations: a depthwise convolution applied to each input channel separately and a pointwise convolution (1x1 convolution) to combine the outputs. This approach minimizes redundancy and enhances efficiency [21].

ShuffleNet: ShuffleNet is developed to address the inefficiencies of traditional CNNs, which introduces two key innovations: pointwise group convolutions and channel shuffling [22]. Pointwise group convolutions reduce computational complexity by processing input channels in groups, while channel shuffling ensures information flow across groups, maintaining model accuracy. These techniques drastically cut down the number of parameters and floating-point operations (FLOPs) without sacrificing performance [23]. The figure 3 illustrates the fully connected (FC) layers of three popular lightweight CNN architectures alongside a feature fusion module.

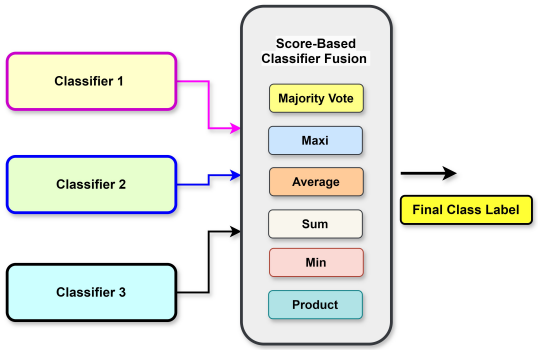


Fig. 4. Score based classifier fusion methods.

### D. Classifier Score Based Fusion Strategies

This work employs three distinct lightweight CNN models can capture unique, complementary aspects of insulator appearance, texture, and contamination patterns. The initial classification is performed using Support Vector Machines (SVMs), a robust baseline classifier, trained independently on the feature sets extracted from each of the three CNNs. Individual classifiers might excel in identifying certain types of contamination or insulator states but falter on others [24]. To overcome these limitations and achieve potentially higher accuracy and robustness, we are implementing a classifier fusion strategy, as depicted in figure 4.

As depicted in figure 4, the score-based classifier fusion algorithm receives the score vectors from all three individual classifiers. Then we apply a specific rule to combine these scores. This study explores six fusion rules: (1) Majority vote (2) Maximum (3) Average (4) Sum (5) Minimum (6) Product. Let $C$ be the total number of classifiers, $M$ be the total number of possible classes, $x$ be the input sample features, and $d_{i,j}(x)$ be the score assigned by the $i$-th classifier to class $\omega_j$ for the input sample $x$. In this equation, $\omega_j$ denotes the $j$-th class label, $\mu_j(x)$ is the combined or fused score for class $\omega_j$ for the input sample $x$, and $\Omega$ is the final predicted class label. Following eqs. (1)-(6) describe score-based classifier fusion rules employed in this work.

$$Majority\,Vote,\ j : \mu_j(x) a = \arg\max_j V_j \tag{1}$$

$$Maximum\,Rule,\ j : \mu_j(x) = \max_{1 \le i \le C} d_{i,j}(x) \tag{2}$$

$$Average\,Rule,\ j : \mu_j(x) = \frac{1}{C} \sum_{i=1}^{C} d_{i,j}(x) \tag{3}$$

$$Sum\ Rule,\ j : \mu_j(x) = \sum_{i=1}^{C} d_{i,j}(x) \tag{4}$$

$$Minimum\ Rule,\ j : \mu_j(x) = \min_{1 \le i \le C} d_{i,j}(x) \tag{5}$$

$$Product\ Rule,\ j : \mu_j(x) = \prod_{i=1}^{C} d_{i,j}(x) \tag{6}$$

The final class label $\Omega$ is typically determined by finding the class $\omega_k$ that maximizes the fused score:

$$\Omega = \arg\max_{\omega_j} \mu_j(x) \tag{7}$$

## III. Experiment Results and Discussions

This research proposes a method for HV power line insulator and contamination classification using classifier decision fusion approach. The validity of this approach is demonstrated through experiments on three independent datasets. Database 1 was primarily designed to evaluate the classification performance for different types of insulator contamination (Clean, Excrement, Salt, Soot). The analysis involved evaluating three lightweight CNN models (MobileNetV2V2, ShuffleNet, EfficientNet-B0) individually and comparing their performance against various score-level classifier fusion techniques. Table I shows the precision, accuracy, sensitivity, F-measure and specificity parameters evaluated using base CNN and best classifier fusion rule on Database 1.

TABLE I
Precision, accuracy, sensitivity, F-measure and specificity parameters evaluated using base CNN and best classifier fusion rule on Database 1.

| Metric / Class | Clean | Excrement | Salt | Soot | Average |
|---|---|---|---|---|---|
| **MobileNetV2** | | | | | |
| Precision | 0.9527 | 0.9601 | 1.0000 | 0.9907 | 0.9758 |
| Sensitivity | 0.9685 | 0.9565 | 0.9926 | 0.9852 | 0.9757 |
| Specificity | 0.9839 | 0.9867 | 1.0000 | 0.9969 | 0.9919 |
| Accuracy | 0.9757 | 0.9757 | 0.9757 | 0.9757 | 0.9757 |
| F-measure | 0.9605 | 0.9583 | 0.9962 | 0.9879 | 0.9757 |
| **ShuffleNet** | | | | | |
| Precision | 0.9612 | 0.9533 | 0.9962 | 0.9851 | 0.9739 |
| Sensitivity | 0.9621 | 0.9630 | 0.9907 | 0.9796 | 0.9738 |
| Specificity | 0.9870 | 0.9842 | 0.9987 | 0.9950 | 0.9912 |
| Accuracy | 0.9738 | 0.9738 | 0.9738 | 0.9738 | 0.9738 |
| F-measure | 0.9616 | 0.9581 | 0.9935 | 0.9823 | 0.9739 |
| **EfficientNet-B0** | | | | | |
| Precision | 0.9687 | 0.9642 | 1.0000 | 0.9981 | 0.9827 |
| Sensitivity | 0.9750 | 0.9722 | 0.9953 | 0.9879 | 0.9826 |
| Specificity | 0.9895 | 0.9879 | 1.0000 | 0.9993 | 0.9942 |
| Accuracy | 0.9826 | 0.9826 | 0.9826 | 0.9826 | 0.9826 |
| F-measure | 0.9719 | 0.9682 | 0.9976 | 0.9930 | 0.9827 |
| **Sum Rule (fusion)** | | | | | |
| Precision | 0.9760 | 0.9715 | 1.0000 | 0.9925 | 0.9850 |
| Sensitivity | 0.9796 | 0.9796 | 0.9926 | 0.9879 | 0.9849 |
| Specificity | 0.9919 | 0.9904 | 1.0000 | 0.9975 | 0.9949 |
| Accuracy | 0.9849 | 0.9849 | 0.9849 | 0.9849 | 0.9849 |
| F-measure | 0.9778 | 0.9756 | 0.9962 | 0.9902 | 0.9850 |

MobileNetV2 model achieved an average accuracy of 97.57% across the four classes. It showed better performance, particularly in identifying 'Salt' contamination with perfect precision (1.0) and high sensitivity (0.9926). However, its precision for 'Clean' (0.9527) and 'Excrement' (0.9601) was slightly lower compared to other classes. The ROC plots as illustrated in figure 5 visually confirm the high true positive rate against a low false positive rate for all classes, indicating good discriminative ability. ShuffleNet attained a slightly lower average accuracy of 97.38%. The average F-measure was 0.9739, and average specificity was 0.9912.

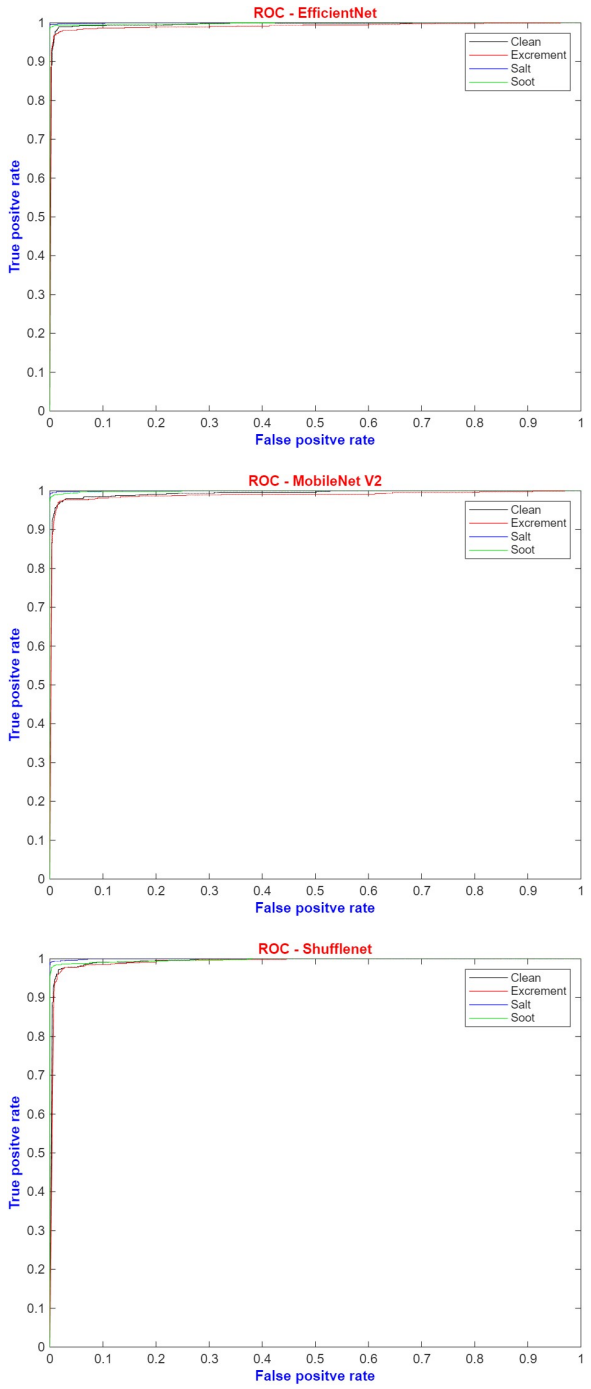


Fig. 5. ROC plots of MobileNetV2, ShuffleNet and EfficientNet-B0 CNN obtained for Database 1.

EfficientNet-B0 model demonstrated the best classification rate among the individual CNNs, achieving an average accuracy of 98.26. It achieved perfect precision for 'Salt' (1.0) and near-perfect precision for 'Soot' (0.9981). The average

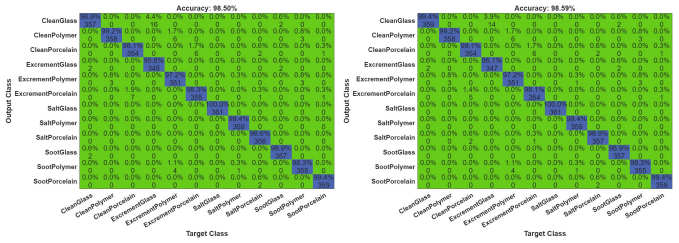


Fig. 6. Confusion matrix obtained using Database 2 shwing top two best accuracy.

F-measure was 0.9827, and average specificity was 0.9942. Moreover, in this study six score-level fusion rules were tested: Majority Vote, Maximum, Average, Sum, Minimum, and Product. The goal was to understand the strengths of the individual classifiers to achieve higher overall accuracy and robustness. The Sum rule emerged as the most effective fusion strategy for Database 1, achieving the highest average accuracy of 98.49%. This represents an improvement over the best individual model (EfficientNet-B0 at 98.26%). The Sum rule improved the average precision to 0.9850, average sensitivity to 0.9849, average specificity to 0.9949, and average F-measure to 0.9850.

While evaluating other fusion rules, the Average rule performed identically to the Sum rule in this case (Accuracy 98.49%). While all fusion rules generally outperformed the individual baseline models (except ShuffleNet compared to the Product rule), the Sum/Average rules provided the most significant boost, demonstrating the benefit of combining classifier scores for this contamination classification task. The experiments on Database 1 clearly indicates the effectiveness of lightweight CNNs for classifying insulator contamination with EfficientNet-B0 as the best performing model. However, employing score-level fusion, particularly the Sum or Average rule, further enhanced the classification accuracy of 98.49%.

Database 2 presented a more complex challenge, requiring the simultaneous classification of both insulator material (Glass - GL, Polymer - PL, Porcelain - PO) and contamination type (Clean - C, Excrement - E, Salt - S, Soot - So), resulting in 12 distinct classes. This synthetic dataset allowed for controlled evaluation across material-contamination combinations as shown in table II. MobileNetV2 achieved an average accuracy of 97.87%. Performance varied slightly across the specific classes. For instance, it achieved perfect precision (1.0) and sensitivity (1.0) for Salt contamination on Glass (SGL) but had lower precision (0.9457) for Clean Glass (CGL). The average F-measure was 0.9787, and average specificity was very high at 0.9980. Figure 6 depicts Confusion matrix obtained using Database 2 shwing top two best accuracy.

Similar to Database 1, the six fusion rules were applied to the scores from the three classifiers trained on Database 2 features. For this 12-class problem, the Maximum fusion rule delivered the best results, achieving an average accuracy of 98.59%. This slightly surpassed the best individual model, EfficientNet-B0 (98.54%). The Maximum rule improved average precision to 0.9860 and maintained high average sensitivity (0.9859), specificity (0.9987), and F-measure (0.9859). The confusion matrix for the Maximum rule (Figure 6(b) ) shows an extremely strong diagonal, indicating highly accurate classification across all 12 combined material and contamination types. The Product rule achieved the next best accuracy at 98.49%. The Average and Sum rules both resulted in 98.40% accuracy, while Majority Vote and Minimum Rule achieved 98.38% accuracy.

The classification task for Database 2 was significantly more complex, despite this, all individual lightweight models performed remarkably well, with accuracies exceeding 97.8%. The application of score-level fusion, with the Maximum rule proving optimal, pushed the average accuracy slightly higher to 98.59%. Again, all fusion methods provided performance close to or better than the best individual model, demonstrating their value in consolidating predictions. The Maximum rule proved most adept at selecting the highest confidence prediction across the classifiers for this specific task.

Database 3 utilized real-world images from the Merged Public Insulator Dataset (MPID), focusing on classifying the insulator material type: Composite, Glass, or Porcelain. This dataset introduced the challenges of real-world variability, including diverse backgrounds, lighting conditions, viewing angles, and weather. Facing real-world data, MobileNetV2 achieved an average accuracy of 97.54% for the 3-class material classification as shown in table III. Its performance was slightly lower for Composite insulators (Sensitivity 0.9278, F-measure 0.9448) compared to Glass and Porcelain. Precision was high for all classes, averaging 0.9711, and specificity was also strong at 0.9863. The ROC plots as shown in figure 7 depicts good separation, but slightly lower for the Composite class curve.

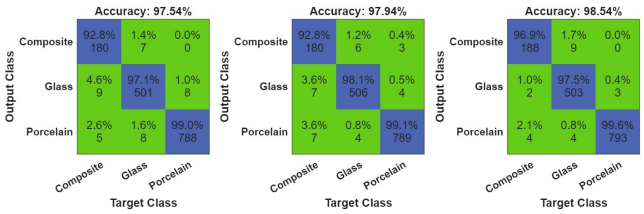


Fig. 7. Confusion matrix plots for Database 3.

ShuffleNet achieved a higher average accuracy of 97.94%. EfficientNet-B0 again delivered the best individual performance on this real-world dataset, with an average accuracy of 98.53%. It showed much more balanced performance across the three material types compared to the other two models. Sensitivity for Composite was significantly improved (0.9690), and it maintained high sensitivity for Glass (0.9748) and Porcelain (0.9962). Average precision (0.9781), specificity (0.9922), and F-measure (0.9790) were all excellent.

The six fusion rules were applied to the outputs of the classifiers trained on the MPID dataset. Consistent with Database 2, the Maximum fusion rule yielded the highest accuracy for Database 3, reaching the best classification rate of 99.26%. This represents a notable improvement over the best individual model (EfficientNet-B0 at 98.53%), demonstrating the significant benefit of fusion on challenging real-world data. The Maximum rule boosted average precision to 0.9907, sensitivity to 0.9890, specificity to 0.9958, and F-measure to 0.9899. This

TABLE II
PERFORMANCE MEASURES EVALUATED USING BASE CNN AND BEST CLASSIFIER FUSION RULE ON DATABASE 2 (12 CLASSES: MATERIAL × CONTAMINATION).

| Metric / Class | CGL | CPL | CPO | EGL | EPL | EPO | SGL | SPL | SPO | SoGL | SoPL | SoPO | Average |
|---|---|---|---|---|---|---|---|---|---|---|---|---|---|
| **MobileNetV2** | | | | | | | | | | | | | |
| Precision | 0.9457 | 0.9724 | 0.9749 | 0.9716 | 0.9695 | 0.9725 | 1.0000 | 1.0000 | 0.9889 | 0.9778 | 0.9780 | 0.9944 | 0.9788 |
| Sensitivity | 0.9667 | 0.9778 | 0.9695 | 0.9501 | 0.9695 | 0.9806 | 1.0000 | 0.9833 | 0.9889 | 0.9778 | 0.9889 | 0.9916 | 0.9787 |
| Specificity | 0.9949 | 0.9974 | 0.9977 | 0.9974 | 0.9972 | 0.9974 | 1.0000 | 1.0000 | 0.9989 | 0.9979 | 0.9979 | 0.9994 | 0.9980 |
| Accuracy | 0.9787 | 0.9787 | 0.9787 | 0.9787 | 0.9787 | 0.9787 | 0.9787 | 0.9787 | 0.9787 | 0.9787 | 0.9787 | 0.9787 | 0.9787 |
| F-measure | 0.9561 | 0.9751 | 0.9722 | 0.9607 | 0.9695 | 0.9765 | 1.0000 | 0.9916 | 0.9889 | 0.9778 | 0.9834 | 0.9930 | 0.9787 |
| **ShuffleNet** | | | | | | | | | | | | | |
| Precision | 0.9779 | 0.9726 | 0.9487 | 0.9724 | 0.9722 | 0.9747 | 1.0000 | 0.9888 | 0.9944 | 1.0000 | 0.9805 | 0.9944 | 0.9814 |
| Sensitivity | 0.9833 | 0.9861 | 0.9750 | 0.9778 | 0.9695 | 0.9612 | 1.0000 | 0.9833 | 0.9861 | 0.9889 | 0.9750 | 0.9889 | 0.9813 |
| Specificity | 0.9979 | 0.9974 | 0.9952 | 0.9974 | 0.9974 | 0.9977 | 1.0000 | 0.9989 | 0.9994 | 1.0000 | 0.9982 | 0.9994 | 0.9983 |
| Accuracy | 0.9813 | 0.9813 | 0.9813 | 0.9813 | 0.9813 | 0.9813 | 0.9813 | 0.9813 | 0.9813 | 0.9813 | 0.9813 | 0.9813 | 0.9813 |
| F-measure | 0.9806 | 0.9793 | 0.9617 | 0.9751 | 0.9708 | 0.9679 | 1.0000 | 0.9861 | 0.9902 | 0.9944 | 0.9777 | 0.9916 | 0.9813 |
| **EfficientNet-B0** | | | | | | | | | | | | | |
| Precision | 0.9514 | 0.9726 | 0.9862 | 0.9773 | 0.9829 | 0.9917 | 1.0000 | 0.9972 | 0.9944 | 0.9944 | 0.9780 | 1.0000 | 0.9855 |
| Sensitivity | 0.9778 | 0.9861 | 0.9916 | 0.9556 | 0.9584 | 0.9944 | 1.0000 | 0.9972 | 0.9916 | 0.9889 | 0.9889 | 0.9944 | 0.9854 |
| Specificity | 0.9954 | 0.9974 | 0.9987 | 0.9979 | 0.9984 | 0.9992 | 1.0000 | 0.9997 | 0.9994 | 0.9994 | 0.9979 | 1.0000 | 0.9986 |
| Accuracy | 0.9854 | 0.9854 | 0.9854 | 0.9854 | 0.9854 | 0.9854 | 0.9854 | 0.9854 | 0.9854 | 0.9854 | 0.9854 | 0.9854 | 0.9854 |
| F-measure | 0.9644 | 0.9793 | 0.9889 | 0.9663 | 0.9705 | 0.9930 | 1.0000 | 0.9972 | 0.9930 | 0.9916 | 0.9834 | 0.9972 | 0.9854 |
| **Maximum Rule (fusion)** | | | | | | | | | | | | | |
| Precision | 0.9573 | 0.9754 | 0.9752 | 0.9886 | 0.9804 | 0.9833 | 1.0000 | 1.0000 | 0.9916 | 1.0000 | 0.9861 | 0.9944 | 0.9860 |
| Sensitivity | 0.9944 | 0.9916 | 0.9806 | 0.9612 | 0.9722 | 0.9806 | 1.0000 | 0.9944 | 0.9889 | 0.9889 | 0.9833 | 0.9944 | 0.9859 |
| Specificity | 0.9959 | 0.9977 | 0.9977 | 0.9989 | 0.9982 | 0.9984 | 1.0000 | 1.0000 | 0.9992 | 1.0000 | 0.9987 | 0.9994 | 0.9987 |
| Accuracy | 0.9859 | 0.9859 | 0.9859 | 0.9859 | 0.9859 | 0.9859 | 0.9859 | 0.9859 | 0.9859 | 0.9859 | 0.9859 | 0.9859 | 0.9859 |
| F-measure | 0.9755 | 0.9835 | 0.9779 | 0.9747 | 0.9763 | 0.9819 | 1.0000 | 0.9972 | 0.9902 | 0.9944 | 0.9847 | 0.9944 | 0.9859 |

TABLE III
PERFORMANCE MEASURES EVALUATED USING BASE CNN AND BEST CLASSIFIER FUSION RULE ON DATABASE 3 (MATERIAL CLASSIFICATION: COMPOSITE, GLASS, PORCELAIN).

| Metric / Class | Composite | Glass | Porcelain | Average |
|---|---|---|---|---|
| **MobileNetV2** | | | | |
| Precision | 0.9625 | 0.9671 | 0.9837 | 0.9711 |
| Sensitivity | 0.9278 | 0.9709 | 0.9899 | 0.9629 |
| Specificity | 0.9946 | 0.9828 | 0.9816 | 0.9863 |
| Accuracy | 0.9754 | 0.9754 | 0.9754 | 0.9754 |
| F-measure | 0.9448 | 0.9690 | 0.9868 | 0.9669 |
| **ShuffleNet** | | | | |
| Precision | 0.9523 | 0.9787 | 0.9862 | 0.9724 |
| Sensitivity | 0.9278 | 0.9806 | 0.9912 | 0.9665 |
| Specificity | 0.9931 | 0.9888 | 0.9845 | 0.9888 |
| Accuracy | 0.9794 | 0.9794 | 0.9794 | 0.9794 |
| F-measure | 0.9399 | 0.9796 | 0.9887 | 0.9694 |
| **EfficientNet-B0** | | | | |
| Precision | 0.9543 | 0.9901 | 0.9900 | 0.9781 |
| Sensitivity | 0.9690 | 0.9748 | 0.9962 | 0.9800 |
| Specificity | 0.9931 | 0.9949 | 0.9887 | 0.9922 |
| Accuracy | 0.9853 | 0.9853 | 0.9853 | 0.9853 |
| F-measure | 0.9616 | 0.9824 | 0.9931 | 0.9790 |
| **Maximum Rule (fusion)** | | | | |
| Precision | 0.9844 | 0.9941 | 0.9937 | 0.9907 |
| Sensitivity | 0.9793 | 0.9903 | 0.9974 | 0.9890 |
| Specificity | 0.9977 | 0.9969 | 0.9929 | 0.9958 |
| Accuracy | 0.9926 | 0.9926 | 0.9926 | 0.9926 |
| F-measure | 0.9819 | 0.9922 | 0.9956 | 0.9899 |

indicates highly accurate and reliable classification of insulator materials even under diverse real-world conditions.

The Product rule achieved the next best accuracy at 99.20%. The Average and Sum rules followed closely with 99.07% accuracy. Majority Vote and Minimum rule achieved 98.80% accuracy. All fusion methods substantially improved upon the individual model accuracies, with the Maximum rule proving most effective at leveraging the highest confidence predictions from the three base classifiers to navigate the complexities of the real-world MPID dataset. This substantial improvement underscores the value of combining predictions from multiple models trained on diverse features to overcome the variability and noise present in real-world inspection images, leading to a highly accurate and reliable insulator material classification system suitable for practical deployment.

TABLE IV
PERFORMANCE COMPARISON OF THE PROPOSED METHOD WITH EXISTING ALGORITHMS.

| Algorithm Ref. | Method | Database | Task | Accuracy (%) |
|---|---|---|---|---|
| [5] | VGG16 | Database1 | Contamination classification | 97.00 |
| [12] | ConvNet | 4125 UAV images | Contamination classification | 85.59 |
| [12] | MobileNetV2 | 4125 UAV images | Contamination classification | 82.80 |
| [11] | CNN | Database1 | Contamination classification | 98.00 |
| Proposed | Classifier fusion | Database1 | Contamination classification | 98.49 |

Table IV provides a comparative assessment of the proposed classifier fusion method against several existing algorithms specifically for the task of insulator contamination classification. The proposed method, when evaluated on Database 1, achieved an accuracy of 98.49%. This performance is benchmarked against four other approaches. The work employing VGG16 on Database 1 reported an accuracy of 97.00% [5]. In another work [11], Convolutional Neural Network based method, also evaluated on Database 1, achieved 98.00% accuracy. These results indicate that the proposed classifier fusion technique slightly outperforms these specific VGG16 and CNN implementations on the same dataset by 1.49% and 0.49%, respectively.

Further comparisons are made against methods tested on different datasets. A ConvNet model [12] tested on 4125 UAV images achieved 85.59% accuracy, and a MobileNetV2 [12] implementation on the same UAV dataset reached 82.80%. While these datasets differ from Database 1, the significantly higher accuracy of the proposed method (98.49%) suggests its potential effectiveness. Overall, the proposed classifier fusion approach demonstrates a competitive, and in some cases superior, performance for contamination classification compared to the listed prior works, particularly when assessed on the same dataset (Database 1).

## IV. CONCLUSIONS

This study addresses the need for accurate and efficient classification of high-voltage insulator contamination and material types. A new framework using the complementary

strengths of three lightweight CNNs (MobileNetV2, ShuffleNet, EfficientNet-B0) combined through score-level classifier fusion is proposed. Experimental evaluations conducted on diverse datasets, including synthetically generated contamination types and materials, as well as challenging real-world images from the MPID dataset, consistently demonstrated the superiority of the fusion approach over individual models. The Sum/Average fusion rule excelled in classifying contamination types (98.49% accuracy), while the Maximum rule proved optimal for the complex 12-class material/contamination task (98.59% accuracy) and robustly classified insulator materials in real-world scenarios (99.26% accuracy). This score-level fusion method effectively mitigates the weaknesses of individual classifiers, leading to a highly accurate, robust, and computationally efficient system suitable for practical deployment in automated power line inspection, thereby enhancing grid maintenance strategies and overall reliability.

## REFERENCES


[1] L. Yang, J. Fan, Y. Liu, E. Li, J. Peng, and Z. Liang, "A review on state-of-the-art power line inspection techniques," *IEEE Transactions on Instrumentation and Measurement*, vol. 69, no. 12, pp. 9350–9365, 2020. [Online]. Available: https://doi.org/10.1109/TIM.2020.3031194

[2] R. A. Bianchi, H. F. Ferraz, R. S. Gonçalves, B. Moura, D. E. Sudbrack, A. Merini, M. de Lourdes G. Machado, R. Pires, and R. Z. Homma, "A synthetic high-voltage power line insulator images dataset," *Data in Brief*, vol. 55, p. 110688, 2024. [Online]. Available: https://www.sciencedirect.com/science/article/pii/S2352340924006553

[3] Y. Liu, D. Liu, X. Huang, and C. Li, "Insulator defect detection with deep learning: A survey," *IET Generation, Transmission & Distribution*, vol. 17, no. 16, pp. 3541–3558, 2023. [Online]. Available: https://ietresearch.onlinelibrary.wiley.com/doi/abs/10.1049/gtd2.12916

[4] X. Liu, X. Miao, H. Jiang, and J. Chen, "Data analysis in visual power line inspection: An in-depth review of deep learning for component detection and fault diagnosis," *Annual Reviews in Control*, vol. 50, pp. 253–277, 2020. [Online]. Available: https://www.sciencedirect.com/science/article/pii/S1367578820300596

[5] H. Ferraz, R. Gonçalves, B. Moura, D. Sudbrack, P. Trautmann, B. Clasen, R. Homma, and R. A. C. Bianchi, "Synthetic images datasets of clean and dirty string insulators used in high-voltage power lines," *Journal of the Brazilian Society of Mechanical Sciences and Engineering*, vol. 46, no. 11, p. 636, 2024. [Online]. Available: https://doi.org/10.1007/s40430-024-05204-2

[6] D. Pernebayeva, D. Sadykova, A. P. James, and M. Bagheri, "Outdoor insulator surface condition evaluation using image classification," in *2018 IEEE International Conference on High Voltage Engineering and Application (ICHVE)*, 2018, pp. 1–4. [Online]. Available: https://doi.org/10.1109/ICHVE.2018.8642233

[7] Z. Zhao, G. Xu, Y. Qi, N. Liu, and T. Zhang, "Multi-patch deep features for power line insulator status classification from aerial images," in *2016 International Joint Conference on Neural Networks (IJCNN)*, 2016, pp. 3187–3194. [Online]. Available: https://doi.org/10.1109/IJCNN.2016.7727606

[8] E. F. S. Filho, R. M. Prates, R. P. Ramos, and J. S. Cardoso, "Power distribution insulators classification using image hybrid deep learning," in *2019 27th European Signal Processing Conference (EUSIPCO)*, 2019, pp. 1–5. [Online]. Available: https://doi.org/10.23919/EUSIPCO.2019.8903139

[9] M. P. Corso, S. F. Stefenon, G. Singh, M. V. Matsuo, F. L. Perez, and V. R. Q. Leithardt, "Evaluation of visible contamination on power grid insulators using convolutional neural networks," *Electrical Engineering*, vol. 105, no. 6, pp. 3881–3894, 2023. [Online]. Available: https://doi.org/10.1007/s00202-023-01915-2

[10] E. Ergun, "Artificial intelligence approaches for accurate assessment of insulator cleanliness in high-voltage electrical systems," *Electrical Engineering*, vol. 107, no. 3, pp. 2969–2982, 2025. [Online]. Available: https://doi.org/10.1007/s00202-024-02691-3

[11] H. Ferraz, R. S. Gonçalves, B. B. Moura, D. E. T. Sudbrack, P. V. Trautmann, B. Clasen, R. Z. Homma, and R. A. C. Bianchi, "Automated classification of electrical network high-voltage tower insulator cleanliness using deep neural networks," *International Journal of Intelligent Robotics and Applications*, vol. 9, no. 3, pp. 818–832, 2025. [Online]. Available: https://doi.org/10.1007/s41315-024-00349-8

[12] A. Serikbay, M. Bagheri, A. Zollanvari, and A. A. Saukhimov, "Cnn-based classification of contaminated high voltage insulator surface," in *2022 IEEE International Conference on Environment and Electrical Engineering and 2022 IEEE Industrial and Commercial Power Systems Europe (EEEIC / I&CPS Europe)*, 2022, pp. 1–5. [Online]. Available: https://doi.org/10.1109/EEEIC/ICPSEurope54979.2022.9854762

[13] S. F. Stefenon, M. P. Corso, A. Nied, F. L. Perez, K.-C. Yow, G. V. Gonzalez, and V. R. Q. Leithardt, "Classification of insulators using neural network based on computer vision," *IET Generation, Transmission & Distribution*, vol. 16, no. 6, pp. 1096–1107, 2022. [Online]. Available: https://ietresearch.onlinelibrary.wiley.com/doi/abs/10.1049/gtd2.12353

[14] R. BENEL MOSTAFA, Badr-Eddine AIT EL HAJ, "Mpid: Merged public insulator dataset," https://zenodo.org/records/14604384, 2025, accessed: October 20, 2025.

[15] R. Jegan, G. K. Birajdar, and S. Chaudhari, "Deep residual multi-resolution features and optimized kernel elm for forest fire image detection using imbalanced database," *Fire Technology*, vol. 61, no. 5, pp. 3323–3349, 2025. [Online]. Available: https://doi.org/10.1007/s10694-025-01729-7

[16] R. Jegan and R. Jayagowri, "Optimized early fusion of handcrafted and deep learning descriptors for voice pathology detection and classification," *Healthcare Analytics*, vol. 6, p. 100369, 2024. [Online]. Available: https://www.sciencedirect.com/science/article/pii/S2772442524000716

[17] O. O. Abayomi-Alli, R. Damaševičius, S. Misra, and A. Abayomi-Alli, "Fruitq: a new dataset of multiple fruit images for freshness evaluation," *Multimedia Tools and Applications*, vol. 83, no. 4, pp. 11 433–11 460, 2024. [Online]. Available: https://doi.org/10.1007/s11042-023-16058-6

[18] G. Seyfi, M. Yilmaz, E. Esme, and M. S. Kiran, "X-ray image analysis for explosive circuit detection using deep learning algorithms," *Applied Soft Computing*, vol. 151, p. 111133, 2024. [Online]. Available: https://www.sciencedirect.com/science/article/pii/S1568494623011511

[19] D. Al-Daloo and P. Bilski, "Classification of music structural functions using deep learning," *International Journal of Electronics and Telecommunications*, vol. 71, no. 3, pp. 1–6, 2025. [Online]. Available: https://doi.org/10.24425/ijet.2025.153608

[20] Z. Xu, H. Shi, P. Lin, and S. Li, "A lightweight model hyperparameters searching method for fast, accurate and on-site lithology identification," *Journal of Rock Mechanics and Geotechnical Engineering*, vol. 17, no. 11, pp. 7023–7037, 2025. [Online]. Available: https://www.sciencedirect.com/science/article/pii/S1674775525001076

[21] T. Zheng, X. Yang, J. Lv, M. Li, S. Wang, and W. Li, "An efficient mobile model for insect image classification in the field pest management," *Engineering Science and Technology, an International Journal*, vol. 39, p. 101335, 2023. [Online]. Available: https://www.sciencedirect.com/science/article/pii/S2215098623000125

[22] H. Mewada and I. M. Pires, "Electrocardiogram signal classification using lightweight dnn for mobile devices," *Procedia Computer Science*, vol. 224, pp. 558–564, 2023, 18th International Conference on Future Networks and Communications / 20th International Conference on Mobile Systems and Pervasive Computing / 13th International Conference on Sustainable Energy Information Technology. [Online]. Available: https://www.sciencedirect.com/science/article/pii/S1877050923011286

[23] A. A. Jabber, G. A. Shadeed, N. Salim, and H. Dibs, "Automated skin lesion diagnosis and classification using k-mean, lab-color-space segmentation and deep learning," *Operations Research Forum*, vol. 6, no. 2, p. 43, 2025. [Online]. Available: https://doi.org/10.1007/s43069-025-00430-3

[24] G. Blinowski and M. Bogucki, "Performance evaluation of selected ml algorithms in gc and aws cloud environments," *International Journal of Electronics and Telecommunications*, vol. 71, no. 4, pp. 1–10, 2025. [Online]. Available: https://doi.org/10.24425/ijet.2025.155471